Applied Surface Science 383 (2016) 283–293

Contents lists available at ScienceDirect

Applied Surface Science

journal homepage: www.elsevier.com/locate/apsusc

Self-assembled monolayers of 1-alkenes on oxidized platinum surfaces as platforms for immobilized enzymes for biosensing

Jose Maria Alonso[a,1], Abraham A.M. Bielen[a,1], Wouter Olthuis[b], Servé W.M. Kengen[c], Han Zuilhof[a,d,*], Maurice C.R. Franssen[a,*]

[a] Laboratory of Organic Chemistry, Wageningen University, Dreijenplein 8, 6703 HB, Wageningen, The Netherlands
[b] BIOS Lab on a Chip Group, MESA+ and MIRA Institutes, University of Twente, P.O. Box 217, 7500 AE Enschede, The Netherlands
[c] Laboratory of Microbiology, Wageningen University, 6703HB Wageningen, The Netherlands
[d] Department of Chemical and Materials Engineering, King Abdulaziz University, Jeddah 22254, Saudi Arabia

ARTICLE INFO

Article history:
Received 10 February 2016
Received in revised form 28 April 2016
Accepted 2 May 2016
Available online 4 May 2016

Keywords:
Self-assembled monolayers
Platinum
Enzyme immobilization
Lactate biosensor

ABSTRACT

Alkene-based self-assembled monolayers grafted on oxidized Pt surfaces were used as a scaffold to covalently immobilize oxidase enzymes, with the aim to develop an amperometric biosensor platform. NH_2-terminated organic layers were functionalized with either aldehyde (CHO) or N-hydroxysuccinimide (NHS) ester-derived groups, to provide anchoring points for enzyme immobilization. The functionalized Pt surfaces were characterized by X-ray photoelectron spectroscopy (XPS), static water contact angle (CA), infrared reflection absorption spectroscopy (IRRAS) and atomic force microscopy (AFM). Glucose oxidase (GOX) was covalently attached to the functionalized Pt electrodes, either with or without additional glutaraldehyde crosslinking. The responses of the acquired sensors to glucose concentrations ranging from 0.5 to 100 mM were monitored by chronoamperometry. Furthermore, lactate oxidase (LOX) and human hydroxyacid oxidase (HAOX) were successfully immobilized onto the PtOx surface platform. The performance of the resulting lactate sensors was investigated for lactate concentrations ranging from 0.05 to 20 mM. The successful attachment of active enzymes (GOX, LOX and HAOX) on Pt electrodes demonstrates that covalently functionalized PtOx surfaces provide a universal platform for the development of oxidase enzyme-based sensors.

1. Introduction

Self-assembled monolayers (SAMs) provide an excellent platform for the development of biosensors. The basic structure of the biosensor comprises a biological recognition element (typically enzymes, nucleic acids or antibodies) that interacts with the analyte, and a transducer which converts that interaction into a quantifiable electronic signal [1,2]. For better precision and reproducibility biosensors often require that the sensing element is immobilized on a solid substrate. SAMs enable the covalent and non-covalent attachment of biomolecules onto surfaces and provide a good control over the accessibility and orientation of the immobilized biomolecules [3,4]. SAMs can be formed on metal substrates to make them compatible with biosensor applications involving current or potential measurements [5]. However, the examples of SAMs on truly conductor materials are practically restricted to thiols on noble metals (Au, Ag, Pt or Pd) [6], and the thermal and hydrolytic stabilities of those SAMs are rather limited.

To overcome such limitations we have recently reported the functionalization of oxidized Pt (PtOx) substrates via the covalent attachment of L-alkenes [7]. In this process, Pt is first oxidized, and upon surface modification yields Pt—O—C linked monolayers. Pt and PtOx are appropriate materials to explore since their extensive use in catalysis, electrochemistry and biosensing [8]. Furthermore, they are compatible with silicon processing in micro and

Abbreviations: SAMs, self-assembled monolayers; RG, reactive group; GOX, glucose oxidase; LOX, lactate oxidase; HAOX, hydroxyacid oxidase; BSA, bovine serum albumin; NHS, *N*-hydroxysuccinimide; TFAAD, trifluoroacetyl-protected 10-amino-1-decene; TFA, trifluoroacetyl; TFEE, 2,2,2-trifluoroethyl undec-10-enoate; TFE, trifluoethyl ester; TAEA, tris-(2-aminoethyl)amine; DIPEA, *N,N*-diisopropylethylamine; DMF, *N,N*-dimethylformamide; DNA, deoxyribonucleic acid; FMN, flavin mononucleotide; SDS-PAGE, sodium dodecyl sulfate- polyacrylamide gel electrophoresis; BS3, bis(sulfosuccinimidyl) suberate sodium salt; DSC, *N,N'*-disuccinimidyl carbonate; HMF, hydroxymethylferrocene; DI, deionized; PBS, phosphate buffered saline; SSC, saline-sodium citrate buffer; GC, gas chromatography; HPLC, high-performance liquid chromatography; FPLC, fast protein liquid chromatography; IRRAS, infrared reflection absorption spectroscopy; XPS, X-ray photoelectron spectroscopy; UHV, ultrahigh vacuum; CA, contact angle; AFM, atomic force microscopy; QCM, quartz crystal microbalance.

* Corresponding authors.
E-mail addresses: han.zuilhof@wur.nl (H. Zuilhof), maurice.franssen@wur.nl (M.C.R. Franssen).

[1] These authors contributed equally to this work.

http://dx.doi.org/10.1016/j.apsusc.2016.05.006
0169-4332/

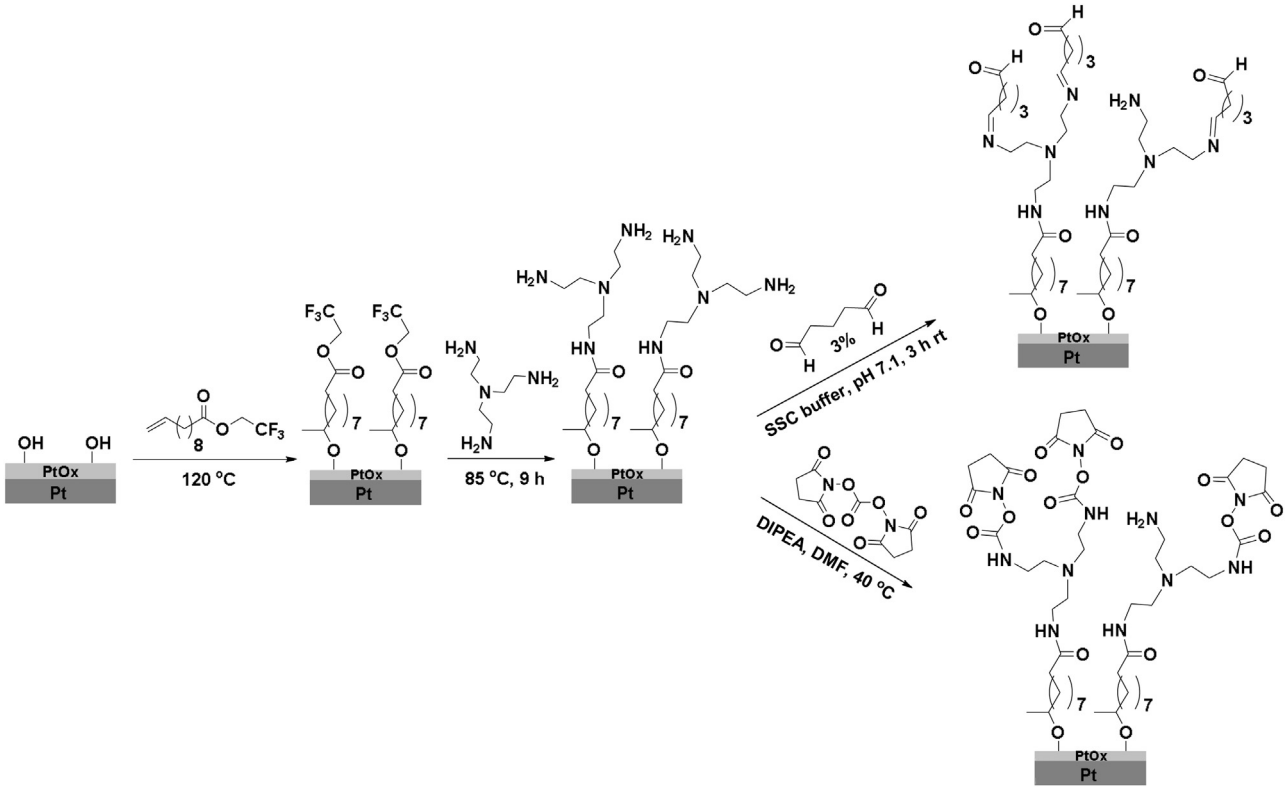

Scheme 1. Route for the functionalization of PtOx with aldehyde (CHO) or *N*-hydroxysuccinimide (NHS) ester groups.

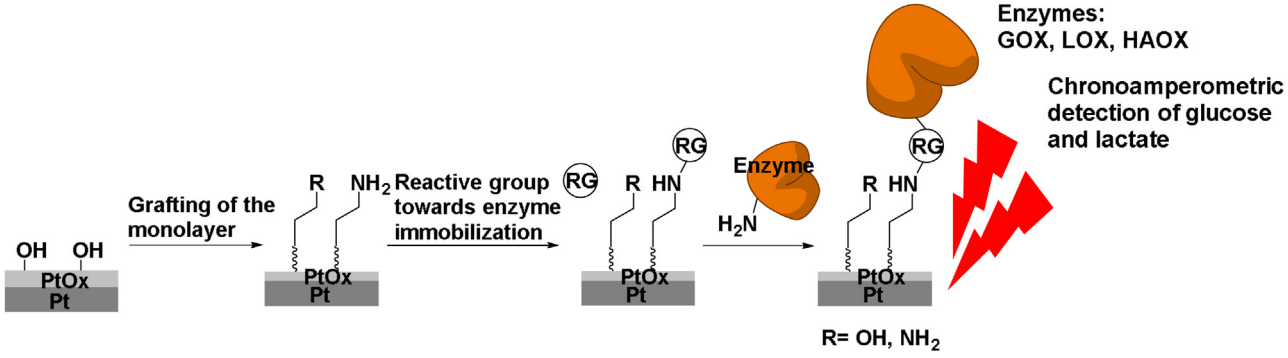

Fig. 1. Overview of the immobilization of enzymes on PtOx for the amperometric sensing of glucose and lactate. Note: RG = reactive group.

nanofabrication techniques, which is not the case for Au [9]. Herein we exploit the potential of this surface modification method for the immobilization of oxidase enzymes such as glucose oxidase (GOX), lactate oxidase (LOX) and human (S)-2-hydroxy-acid oxidase (HAOX) on functionalized Pt electrodes (Fig. 1). These enzymes were selected because their substrates, glucose and lactate, are important analytical targets in biomedical and industrial applications [10–12]. No assay is performed more frequently than that for glucose, as the global prevalence of diabetes approaches 10% among adults aged 18 years and above [13]. On the other hand lactate levels are used as biomarker for physical exercise and for several pathological conditions: cardiogenic shock, renal failure and tissue hypoxia [12].

The activity of immobilized enzymes was assessed by chronoamperometry according to the reactions depicted in Eqs. (1)–(3). First, glucose or lactate is oxidized enzymatically: glucose oxidase (GOX, Eq. (1)) catalyzes the oxidation of glucose to gluconolactone, while lactate oxidase (LOX, Eq. (2)) and (S)-2-hydroxy-acid oxidase (HAOX Eq. (2)) catalyze the conversion of lactate to pyruvate. The O_2 required in the oxidation process is reduced, resulting in the formation of hydrogen peroxide (H_2O_2). Finally, electrochemical oxidation (Eq. (3)) of the enzymatically produced H_2O_2 at these electrodes is used to generate a quantifiable electronic signal. Unlike for gold electrodes, which need an electron mediator to facilitate electron transfer from the enzyme to the electrode, H_2O_2 can be detected directly using Pt electrodes.

$$\beta\text{-D-glucose} + O_2 \rightarrow \text{D-glucono-1,5-lactone} + H_2O_2 \quad (1)$$

$$\text{L-lactate} + O_2 \rightarrow \text{pyruvate} + H_2O_2 \quad (2)$$

$$H_2O_2 \rightarrow O_2 + 2H^+ + 2e^- \quad (3)$$

In the current paper different enzyme coupling methods were tested. Electrode surfaces were characterized by static contact angle (CA), infrared reflection absorption spectroscopy (IRRAS), X-ray photoelectron spectroscopy (XPS) and atomic force microscopy (AFM). Our results show the successful immobilization of active oxidase enzymes (GOX, LOX and HAOX) on Pt electrodes. Moreover,

they demonstrate that covalent functionalized Pt oxide surfaces offer a promising platform for the fabrication of biosensors.

2. Experimental

2.1. Chemicals

2,2,2-Trifluoroethyl undec-10-enoate (TFEE) [14] and trifluoroacetyl-protected 10-amino-1-decene (TFAAD) [15] were synthesized as described elsewhere. Tris-(2-aminoethyl)amine (TAEA, 98%) was obtained from TCI Chemicals. Glutaraldehyde 50% aq. solution was supplied by Alfa Aesar. *N,N*-Di*iso*propylethylamine (DIPEA, biotech grade, 99.5%), *N,N*-dimethylformamide (DMF, anhydrous, 99.8%), sodium citrate tribasic dihydrate (≥99%) and bis(sulfosuccinimidyl) suberate sodium salt (BS3, ≥95%) were purchased from Sigma Aldrich. *N,N'*-Disuccinimidyl carbonate (DSC, 98%), 5-hexen-1-ol (99%) and NaCl (99.5%) were provided by Acros Organics. Acetone, ethanol and CH_2Cl_2 were obtained from Sigma-Aldrich (HPLC grade). Deionized (DI) water was used from a Milli-Q Integral water purification system (Merck-Millipore, USA). Phosphate buffer (200 mM, pH 7) was prepared from a solution of KH_2PO_4 (p.a., Merck KGaA) in DI water. Saline-sodium citrate buffer (SSC, pH 7.1) consisted of 0.15 M NaCl and 0.015 M sodium citrate tribasic solution. Bovine serum albumin (BSA, lyophilized powder, ≥98%), glucose oxidase (GOX from *Aspergillus niger*, lyophilized powder, ~200 U/mg) and lactate oxidase (LOX, from *Pediococcus sp*, lyophilized powder, ≥20 units/mg solid) were obtained from Sigma Aldrich. Human hydroxyacid oxidase (HAOX) was cloned and expressed in *Escherichia coli* and isolated as described in the supplementary data.

2.2. Preparation of oxidized platinum (PtOx) substrates

200 nm thick platinum films were sputtered over 6 μm thermal silicon oxide on silicon wafers, using 10 nm Ta as adhesion layer. Pt pieces (1×1 or 1×2.5 cm^2 for infrared reflection absorption spectroscopy-IRRAS) were cleaned by sonication in acetone and CH_2Cl_2 for 5 min each. Subsequently, Pt surfaces were oxidized by exposure to oxygen plasma (0.1 mbar, 15 sccm, 50 W, Plasma System ATTO Diener, Germany) for 30 min and stored in an Ar-glovebox until further use.

2.3. Functionalization of PtOx surfaces

2.3.1. Covalent attachment of TFEE to PtOx substrates

Neat TFEE (1.5–2 mL) was added to a three necked flask equipped with a capillary, a reflux condenser and connected to a vacuum pump. This setup was degassed for 30 min by gentle Ar flow at 120 °C under 20 mbar pressure. Subsequently, freshly oxidized Pt surfaces were transferred to the reaction flask and heated at 120 °C under a low Ar flow for 16 h at 20 mbar pressure. Modified Pt surfaces were removed from the solution, rinsed with CH_2Cl_2, and sonicated twice in this solvent for 3 min. At last, the samples were dried with a stream of Ar and stored in a glovebox.

2.3.2. Covalent attachment of 5-hexen-1-ol/TFAAD mixed monolayers to PtOx surfaces

A mixture of neat 5-hexen-1-ol (1.7 mL) and TFAAD (0.35 mL) was added to the above mentioned setup. The system was degassed for 30 min by Ar flow at 90 °C under 35 mbar pressure. Next, freshly oxidized Pt surfaces were transferred to the reaction flask and heated at 90 °C under a low Ar flow for 16 h at 35 mbar pressure. The functionalized Pt surfaces were removed from the solution, rinsed thoroughly with CH_2Cl_2, and sonicated twice in this solvent for 3 min. At last, the samples were dried with a stream of Ar and stored in a glovebox.

2.3.3. Reaction of TFE surfaces with tris-aminoethylamine (TAEA)

The TFE-terminated surfaces (typically 2 samples 2×1.5 cm) were transferred to a flask containing TAEA (5 mL) and left to react under Ar atmosphere for 9 h at 85 °C. The samples were then rinsed with EtOH and sonicated in EtOH and CH_2Cl_2 for 3 min each. Subsequently, the surfaces were dried with a stream of Ar and stored in the glovebox until further use.

2.3.4. Deprotection of TFAAD group

The 5-hexen-1-ol/TFAAD mixed monolayer surface was exposed to an aqueous 1 M NaOH solution for 30 s. The sample was then rinsed with H_2O, CH_2Cl_2 and sonicated for 1 min in CH_2Cl_2. The OH-/NH_2-terminated surface was directly subjected to further functionalization.

2.3.5. Functionalization of NH_2- surfaces with aldehyde (CHO) moieties

NH_2-terminated surfaces were covered with 150 μL of a 3% solution of glutaraldehyde in SSC buffer for 3 h at room temperature, rinsed thoroughly with DI water and sonicated in CH_2Cl_2 for 3 min. The CHO-functionalized surfaces were immediately used for enzyme immobilization.

2.3.6. Functionalization of NH_2-surfaces with NHS groups

NH_2-terminated surfaces were immersed in a 5 mL solution of DSC (0.1 M) and DIPEA (0.1 M) in dry DMF for 16 h at 40 °C. Subsequently, the samples were rinsed thoroughly with DMF and sonicated in CH_2Cl_2 for 3 min. Only freshly prepared NHS-terminated surfaces were employed for enzyme immobilization.

2.3.7. Enzyme/protein immobilization protocols

Method A. The CHO- (or CO–NHS) terminated surface was covered with 100 μL of a 3 mg/mL solution of GOX or LOX or BSA in 0.2 M phosphate buffer (pH 7) for 3 h at room temperature. Then the sample was rinsed thoroughly with phosphate buffer and immediately subjected to further analysis.

Method B. 100 μL of freshly prepared solution of GOX (10, 20 or 50 mg/mL) in 25% glutaraldehyde in SSC buffer were spotted on a CHO-functionalized surface and left on the sample for 3 h at room temperature. Subsequently, the enzyme containing sample was rinsed thoroughly with 0.2 M phosphate buffer and analyzed directly afterwards.

Method C. An OH-/NH_2- mixed monolayer surface was covered with 100 μL of a 4.4 mM solution of bis(sulfosuccinimidyl) suberate sodium salt (BS3) in 0.05 M phosphate buffer (pH 7) for 15 min at room temperature. Afterwards, the sulfo-NHS-functionalized surface was rinsed with 0.05 M phosphate buffer and covered with 100 μL of a 3 mg/mL solution of LOX for 45 min. Finally the sample was rinsed thoroughly with 0.2 M phosphate buffer and analyzed immediately.

Method D. Layer by layer approach: the CHO- (or CO–NHS) terminated surface was covered with 100 μL of a 1 mg/mL solution of HAOX in 0.2 M phosphate buffer (pH 7) for 1 h at room temperature. Subsequently, the sample was rinsed thoroughly with 0.2 M phosphate buffer and covered with 100 μL of 3% glutaraldehyde in SSC buffer for 1 h at room temperature. After rinsing with SSC buffer, the HAOX attachment and glutaraldehyde coupling steps were repeated once. The HAOX immobilization protocol was completed with a final HAOX attachment step.

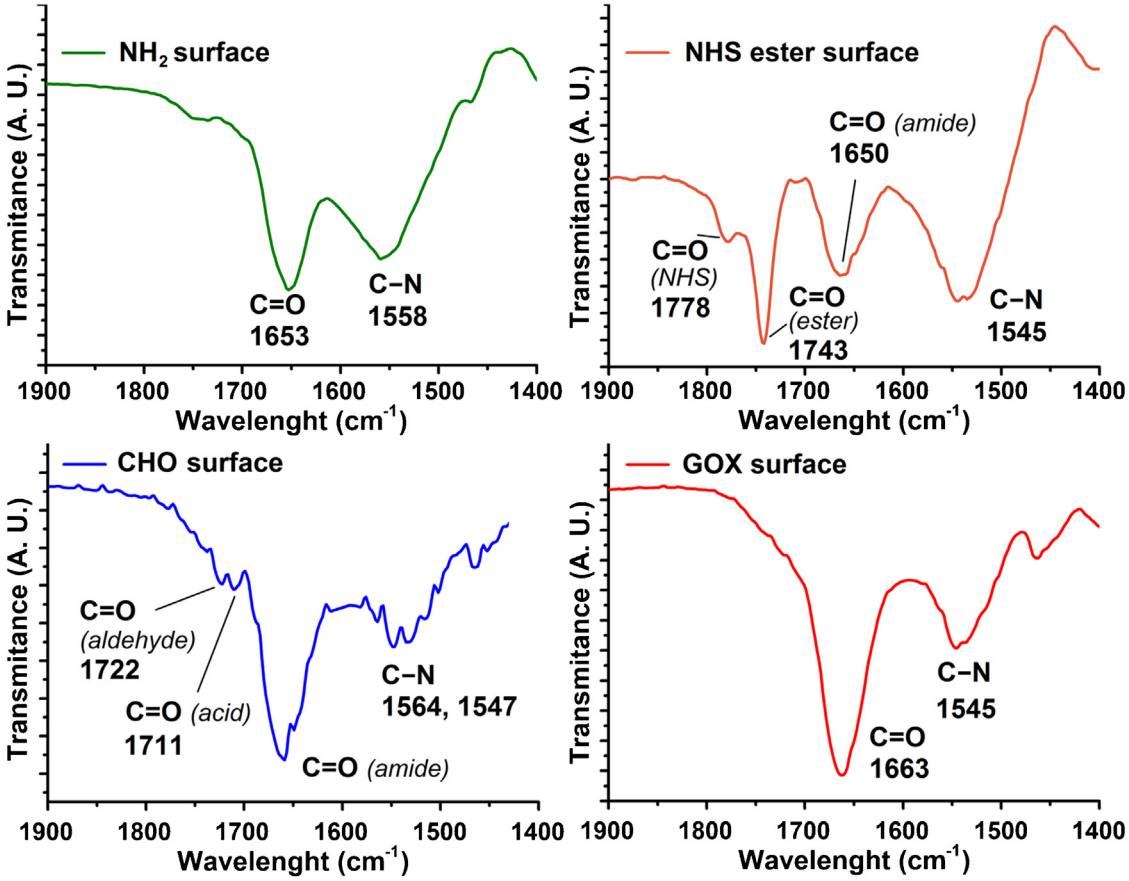

Fig. 2. IRRAS spectra in the 1900–1400 cm^{-1} region for NH_2–, NHS-ester, CHO- and GOX-functionalized surfaces. GOX surface was prepared by immobilization of GOX onto a CHO-activated sample.

2.4. Instrumentation

2.4.1. X-ray photoelectron spectroscopy (XPS) measurements

The X-ray photoelectron spectroscopy (XPS) analysis of surfaces was performed using a JPS-9200 Photoelectron Spectrometer (JEOL, Japan). Survey and high-resolution spectra were obtained under UHV conditions using monochromatic Al Kα X-ray radiation at 12 kV and 20 mA, and an analyzer passes energy of 50 eV for wide scans and 10 eV for narrow scans. The emitted electrons were collected at 10° from the surface normal. All XPS spectra were evaluated by Casa XPS software (version 2.3.15). Survey spectra were corrected with linear background before fitting, whereas high-resolution spectra were corrected with Shirley background. Atomic area ratios were determined after a baseline correction and normalizing the peak area ratios by the corresponding atomic sensitivity factors (1.00 for C_{1s}, 1.80 for N_{1s}, 2.93 for O_{1s}, 4.43 for F_{1s}, 15.5 for Pt_{4f}). XPS survey scan data were employed to calculate the thickness d of the alkyl layer using Eq. (4) [16,17],

$$d = -\lambda_{Pt4f} \cos\gamma \ln(Pt_{4f}^{Grafted}/Pt_{4f}^{Ox}) \quad (4)$$

where $Pt_{4f}^{Grafted}$ = atomic concentration of Pt derived from the Pt_{4f} signal for the grafted layer, Pt_{4f}^{Ox} = atomic concentration of Pt derived from the Pt_{4f} signal for the bare PtOx surface, λ = attenuation length of the Pt_{4f} electrons in the hydrocarbon layer (4.01 nm) and γ = electron take-off angle relative to the sample surface normal (10°).

2.4.2. Static water contact angle (CA) measurements

The wettability of the modified surfaces was determined by automated static water contact angle measurements with a Krüss DSA 100 goniometer (volume of the drop of deionized water was 3.0 μL). The reported values are the average of at least 2 droplets and the relative error is less than ±3°.

2.4.3. Infrared reflection absorption spectroscopy (IRRAS)

IRRAS spectra were obtained with a Bruker Tensor 27 FT-IR spectrometer, using a commercial variable-angle reflection unit (Auto Seagull, Harrick Scientific). A Harrick grid polarizer was installed in front of the detector and was used for measuring spectra with p-polarized radiation with respect to the plane of incidence at the sample surface. Single channel transmittance spectra were collected at 80° using 2048 scans in each measurement. The data recorded on a freshly cleaned reference Pt oxide surface were subtracted from the raw data for the modified surfaces, after which a baseline correction was applied to give the reported spectra.

2.4.4. Atomic force microscopy (AFM) characterization

AFM images (1 × 1 and 5 × 5 μm^2) were obtained with a MFP3D AFM (Asylum Research, Santa Barbara, CA) at a scan speed of 50.08 μm/s at a resolution of 512 × 512 pixels. The imaging was performed in air in tapping mode using OLYMPUS OMCL-AC240TS-R3 microcantilevers with a spring constant of 2 N/m. Images were flattened with a first order using the MFP3D software.

2.4.5. Detection of enzymatic activity by chronoamperometry

The enzymatic activities of the immobilized GOX were evaluated by monitoring substrate concentration dependent hydrogen peroxide (H_2O_2) formation using chronoamperometry. Chronoamperometric measurements were performed with a Potentiostat (PGstat100, controlled by NOVA software, Metrohm Autolab, U.K.)

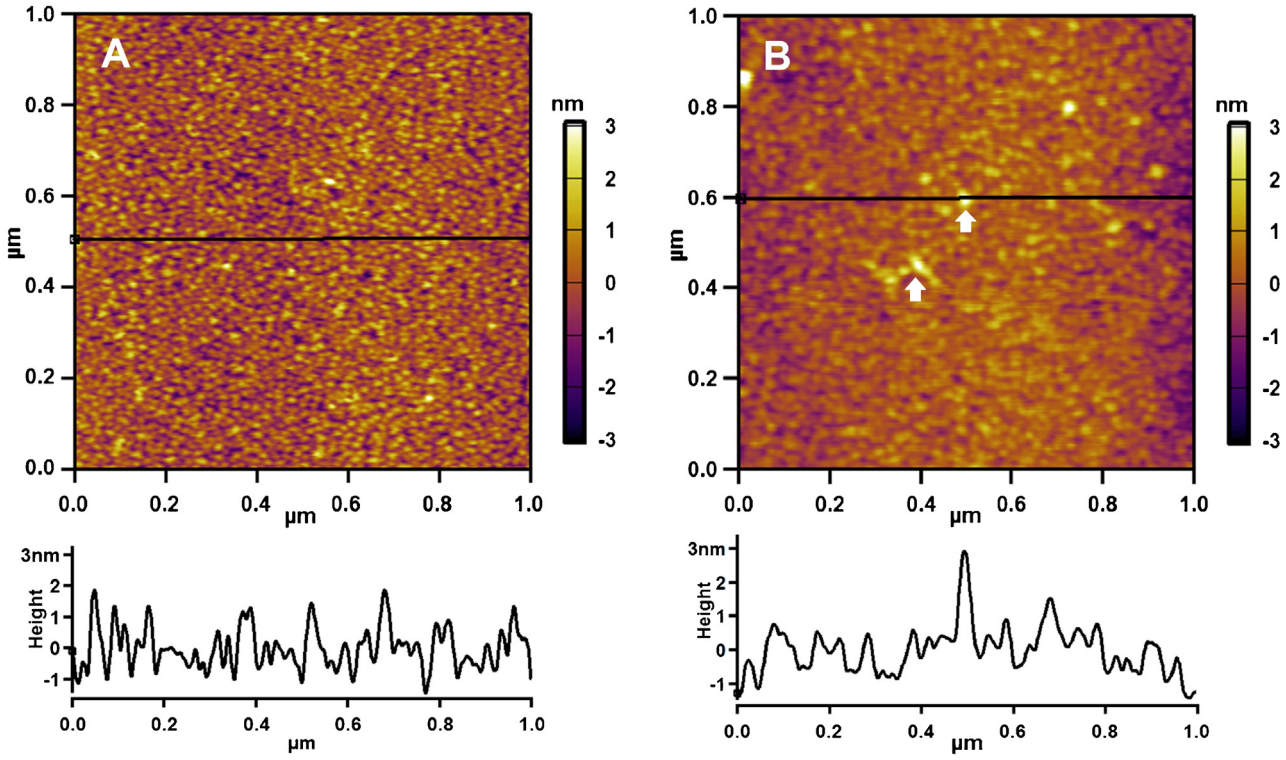

Fig. 3. A: tapping AFM image CHO-functionalized PtOx (scan sizes of 1 × 1 μm, rms roughness 0.80 nm); B: tapping AFM image of GOX immobilized onto CHO-terminated monolayer (scan size of 1 × 1 μm, rms roughness 0.55 nm). White arrows point to irregular aggregates on the surface.

equipped with (i) a platinum wire counter electrode (MW-1033, BASi, USA) (ii) an Ag/AgCl reference electrode (MF-2052, RE-5B, BASi, USA) and, (iii) platinum covered slides, modified with the enzyme/monolayer system, as working electrodes (surface-liquid contact area: 1 cm^2). Platinum surfaces were contacted via a copper tape to the potentiostat using an electrical clamp. Experiments were performed in 0.2 M potassium phosphate buffer, pH 7.0 at room temperature (20 ± 2 °C), with either glucose (0–100 mM) or lactate (0–20 mM). Chronoamperometric measurements were started directly after substrate addition. A two second period (0 V) preceded a single potential step (0.5 V vs Ag/AgCl, 10 s). Currents measured 10 s after the potential step initiation were used for further analysis. PtOx monolayer surfaces decorated with GOX, LOX and HAOX were analyzed in this way; CHO- and BSA-terminated surfaces served as blanks. Experiments were carried out in duplicate, i.e. two PtOx samples modified by the same protocol were tested independently. In addition acquired chronoamperometric data were fitted using the Michaelis–Menten enzyme kinetic model: $y = V_{max} \times x/(K_M + x)$, with x being the substrate concentration and y the recorded current densities.

3. Results and discussion

3.1. Preparation of CHO- and NHS ester-functionalized monolayers on PtOx

Pt films were functionalized with aldehyde (CHO) or *N*-hydroxysuccinimide (NHS) ester groups to provide an anchoring point for the immobilization of GOX (Scheme 1). For this, PtOx surfaces were produced by oxygen plasma treatment (0.1 mbar, 15 sccm O_2, 50 W) of 200 nm-thick Pt films for 30 min [7]. Functionalization of PtOx surfaces with trifluoroethyl undec-10-enoate (TFEE) afforded ester-terminated layers [7]. This alkene was chosen because the terminal trifluoroethyl ester (TFE) moiety is a versatile group for chemical transformations, also on surfaces [18].

Subsequently, the TFE-functionalized layer was converted into an NH_2-terminated surface by reaction with tris-(2-aminoethyl)amine (TAEA) at 85 °C for 9 h. The static water contact angle (CA) decreased from 79 ± 2° to 52 ± 2°, which corroborates the formation of a more hydrophilic surface. X-ray photoelectron spectroscopy (XPS) also confirmed the grafting of the surface with NH_2- moieties (Fig. S1). The XPS survey scan displayed the distinct N peak at about 400 eV (Fig. S1A). Moreover, the attenuation of the electrons emitted from the bulk Pt [16,17] allowed to estimate an increase of ~0.6 nm in the thickness of the monolayer after reaction with TAEA. The XPS wide scan-derived surface atomic composition shows the presence of 3% F, which indicates that ~25% of TFE groups remain unreacted on the surface. The contribution of grafted TFEE molecules was subtracted in further calculations based on XPS survey and narrow scan spectra (Fig. S1). The XPS wide scan-derived corrected C/N ratio was calculated to be 4.4. This value indicates that the attachment of TAEA onto the TFE-functionalized surface occurs preferentially through a single amine moiety (theor. ratio 4.2), as coupling via two amine groups in a bridge conformation would afford a theoretical ratio of 7.0. The XPS narrow scan spectrum of the C_{1s} region displays three main contributions (Fig. S1B) at 285.1, 286.2 and 288.2 eV corresponding to alkyl carbon (C—C), carbon atoms bound to oxygen (C—O) or nitrogen (C—N), and the carbon atom in the amide group (NH—C=O), respectively. The experimental corrected ratio of C—C/(C—O,C—N) is 1.4, which again suggests that the coupling of TAEA via a single amine group (theoretical ratio 1.3) is favored over the attachment of two amine moieties in a bridge conformation (theoretically expected ratio C—C/(C—O/C—N) is 2.0). Infrared reflection absorption spectroscopy (IRRAS) spectrum displays the N—H stretching peak of the NH_2 group at 3277 cm^{-1} (Fig. S1E). The C=O stretching area possesses a major peak at 1653 cm^{-1} (Fig. 2) belonging to the carbonyl of the

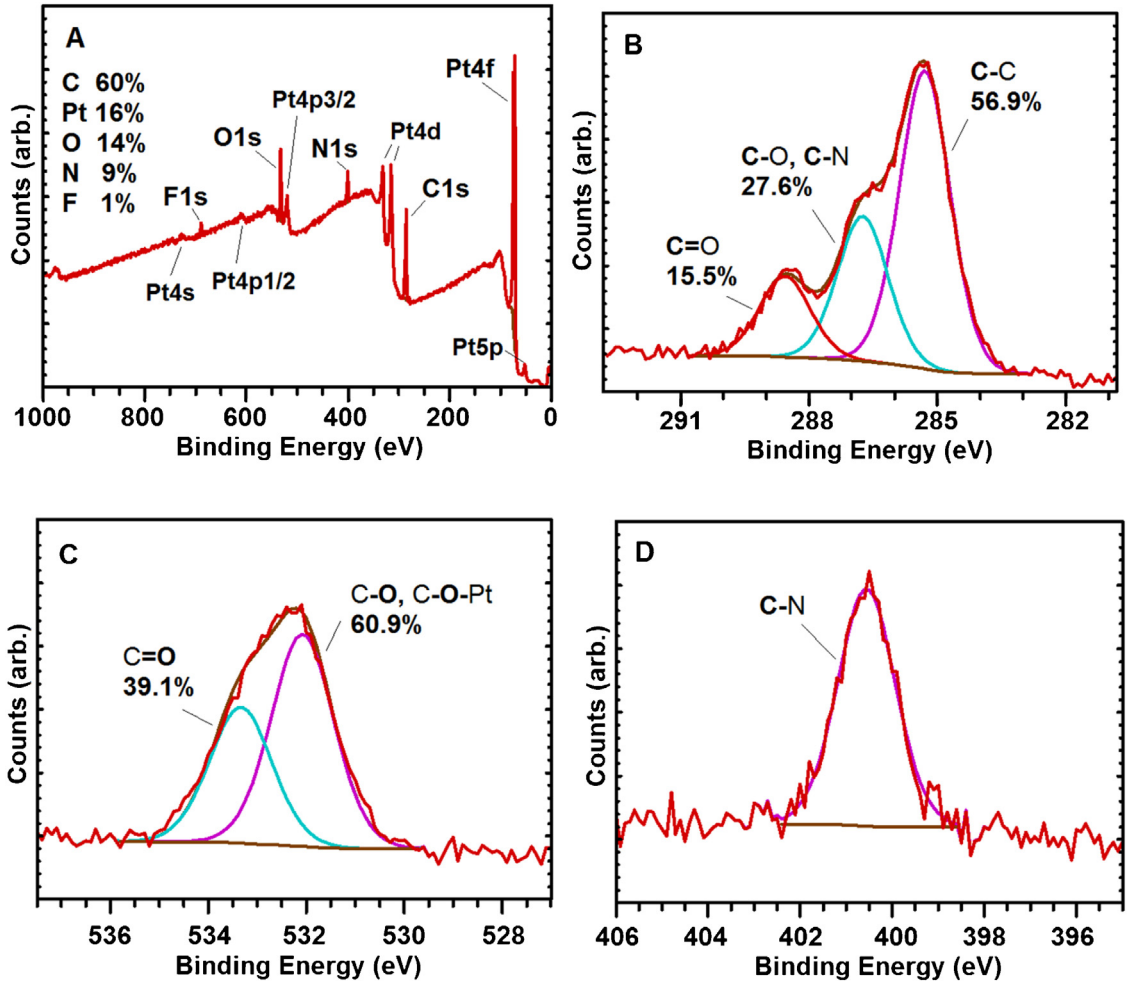

Fig. 4. (A) XPS survey, (B) C_{1s}, (C) O_{1s} and (D) N_{1s} narrow scan of GOX monolayer-functionalized surface.

amide bond (amide I), while the C—N stretching (amide II band) appears at 1558 cm^{-1}. The shoulder signal at 1750 cm^{-1} might correspond to the combined contribution of the carbonyl signal of the TFE layer and of the hydrolyzed TFE ester. If separate, the TFE ester carbonyl is expected at 1761 cm^{-1} and the carboxylic acid carbonyl at 1710–1745 cm^{-1} [18,19].

Functionalization of the surface with aldehyde (CHO) groups occurred by reaction of the NH_2-terminated layer with glutaraldehyde (GA) at room temperature in buffered solution, yielding an increase in the static water CA from $52 \pm 2^\circ$ to $69 \pm 3^\circ$. In addition, XPS analysis reveals an attenuation of the Pt_{4f} electrons emitted from the bulk Pt, which corresponds to an increase of ~0.7 nm in the monolayer thickness (Table S2 and Fig. S2). The IRRAS spectrum exhibits two new bands in the C=O stretching region (Fig. 2). The peak at 1722 cm^{-1} is attributed to the free CHO moiety, whereas the band at 1711 cm^{-1} would correspond to COOH moieties produced by the air oxidation of the aldehyde group and by the hydrolysis of non-reacted TFE ester groups [19,20]. An AFM topography picture of CHO-functionalized organic layers over a scan size of 1×1 μm (Fig. 3a, rms roughness 0.80 nm) shows a homogeneous surface without aggregates. Besides, the AFM micrograph reveals that the organic layer is conformal to the Pt surface, since the typical topography features of Pt are still well visible [21]. The rms roughness values of the CHO-functionalized surface decrease slightly when compared to the PtOx surface (rms roughness 1.1 nm, Fig. S3), which indicates the formation of a cushioning monolayer.

NHS-ester terminated monolayers were produced via coupling of the NH_2-functionalized surface with *N,N'*-disuccinimidyl carbonate at 45 °C in DMF. DIPEA was added to buffer the reaction medium. Grafting of the NHS-ester moieties increased the static water CA from $52 \pm 2^\circ$ to $66 \pm 2^\circ$. The occurrence of NHS groups was confirmed as well by XPS (Fig. S4). Deconvolution of the carbonyl region of the narrow scan C_{1s} spectrum (287–289 eV) provides two components at 288.1 and at 289.3 eV, which correspond to the NH—C=O and to the N—(C=O)$_2$ of the NHS group [22], respectively. Moreover, calculation of the thickness indicates a slight increase of 0.3 nm. Characterization of the surface by IRRAS reveals the appearance of diagnostic C=O stretching vibrations at 1778 and 1741 cm^{-1} (Fig. 2) that are associated to the cyclic imide and to the ester group of the pendant CO—NHS moiety, respectively [23].

3.2. Immobilization of GOX and chronoamperometric assessment of GOX activity

Two immobilization strategies were applied to covalently attach GOX to CHO-functionalized Pt surfaces. This resulted in the formation of a GOX monolayer (method A) and GOX crosslinked surfaces (method B).

3.2.1. Covalent attachment of a GOX monolayer according to Section 2.3.7 (method A)

Immobilization of glucose oxidase (GOX) was accomplished by incubation of the activated surface with enzyme solution (3 mg/mL) for 3 h at room temperature. Overall CHO- and NHS ester-functionalized layers afford the same results in terms of enzyme attachment. Given these results and the fact that

introducing CHO groups is simpler and less time consuming than creating NHS ester groups, CHO-terminated surfaces were preferentially used for fabrication and characterization of the sensor platform. The static water CA changed from 69 ± 3° (CHO surface) to 64 ± 1° after GOX immobilization. Characterization of the enzyme-containing organic layer by XPS shows an attenuation of the Pt_{4f} electrons emitted from the bulk Pt which corresponds to a "dried" GOX layer thickness of ~2.3 nm. This value was used to estimate a surface enzyme loading $\Gamma \sim 2.0$ pmol cm^{-2} according to Eq. (5) [24].

$$\Gamma = d\rho M^{-1} \quad (5)$$

where d is the thickness of the enzyme layer, ρ = density of the enzyme (1.35 g cm^{-3} for proteins) [25], M = Molar mass of GOX (160×10^3 g mol^{-1}). Eq. (5) was applied considering that for protein monolayers the thickness value obtained by XPS is comparable to that estimated in literature by optical methods such as ellipsometry [26]. It must be noted that XPS measurements are performed in UHV conditions (10^{-7} Pa) whereas optimal measurements to determine enzyme coverage can typically be done in the swollen state of the protein in aqueous environment, i.e. by quartz crystal microbalance (QCM) [27]. The calculated enzyme loading (2.0 pmol cm^{-2}) is close to literature data for GOX on NHS-functionalized mercaptopropionic acid SAMs on Au (1.9 pmol cm^{-2}) [27]. The XPS C_{1s} narrow scan could be fitted with three distinctive components. The peaks at 285.3, 286.7, and 288.6 eV belong correspondingly to C—C, C—O & C—N, and to C=O atoms present in the monolayer and in the immobilized GOX (Fig. 4) [28]. Deconvolution of the O_{1s} region provides two peaks. The signal at 532.1 eV is attributed to oxygen atoms in C—O and Pt—O—C groups, while the peak at 533.3 eV is associated to C=O moieties [29]. The IRRAS spectrum exhibits the N—H stretching vibration of the amide bond in the polypeptide chain at 3319 cm^{-1}. The amide I (C=O stretching) and amide II (C—N stretching plus N—H in plane) bands appear at 1663 and 1545 cm^{-1}, respectively (Fig. 5) [30].

AFM analysis of covalently attached GOX onto CHO-terminated organic layers shows a uniform surface with a few aggregates of GOX [27] over a scan size of 1 × 1 μm (Fig. 3b, rms roughness 0.55 nm). The typical dotted topography of sputtered Pt remains the same, which suggests that immobilized GOX molecules are conformal to the Pt surface. Moreover, GOX-containing surfaces exhibit rms roughness values again lower than that of the CHO surface (Fig. 3a, rms roughness 0.80 nm), indicating that immobilized enzymes form a cushioning layer.

3.2.2. Immobilization and crosslinking of GOX (Section 2.3.7, method B)

In order to enhance the loading of enzyme, CHO-terminated layers were incubated with crosslinked GOX solutions (10, 20 and 50 mg/mL in 25% glutaraldehyde solution). XPS characterization of the surfaces shows an increase in the layer thickness of 3.9 ± 0.6, 4.2 ± 1.2 and 4.7 ± 2.7 nm respectively when compared to CHO-functionalized surface (Fig. S5). The relatively large standard deviation of the thickness values suggests a low reproducibility of this immobilization approach. Crosslinking of the enzyme created irregular aggregates with sizes that depend on the enzyme concentration. In this regard AFM micrographs showed up to ~100 × 100 nm sized GOX aggregates for 10 mg/mL GOX concentration, whereas a 50 mg/mL GOX solution produced 300 × 300 nm sized aggregates (Fig. S6).

3.2.3. Chronoamperometric analysis of GOX-functionalized PtOx surfaces

The enzymatic activity of the covalently attached GOX enzymes was evaluated by chronoamperometry for glucose concentrations up to 100 mM. During the chronoamperometric measurement

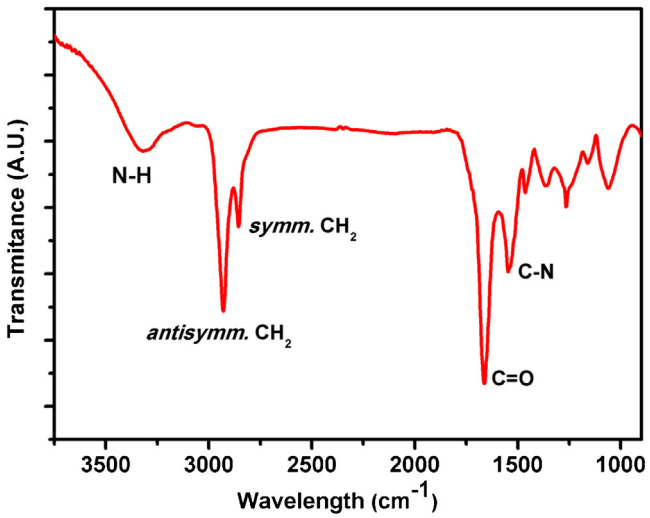

Fig. 5. IRRAS spectrum of GOX monolayer-functionalized surface.

immobilized GOX catalyzes the conversion of glucose to gluconolactone. The O_2 required for this process is thus reduced to H_2O_2. Finally, the enzymatically generated H_2O_2 is oxidized electrochemically at 0.5 V on the PtOx surface producing a quantifiable electronic signal (current). Additionally, CHO-terminated PtOx surfaces and BSA-monolayer surfaces (Fig. S7), which served as non-catalytic controls, were tested to investigate the effect of a monolayer and of an immobilized protein respectively on the electrochemical measurements.

For all analyzed surfaces repetitive blank measurements (no substrate added) revealed steady background signals. For glucose concentrations of 50 mM a current density of ~0.2 μA/cm^2 was observed for the non-catalytic CHO-terminated surface, and of ~0.06 μA/cm^2 for the BSA-monolayer surfaces (Fig. 6). The observed currents are likely the result of non-enzymatic glucose oxidation at the Pt surface, a process that has been reported previously [31]. On average, the measured currents for the BSA-monolayer were lower than for the CHO-terminated surfaces (Fig. 6). This result suggests that BSA protein attachment suppresses glucose diffusion to the surface.

The detected currents for the immobilized GOX surfaces (Fig. 6) were significantly higher compared to the non-catalytic controls, indicating the successful attachment of active GOX enzyme to the CHO-functionalized Pt surfaces. Furthermore, these results show that GOX enzymes immobilized on SAMs grafted onto PtOx work as a real biosensor for glucose.

The GOX biosensors response currents showed the shape of a saturation curve with a dynamic range from 0.5 to 50 mM glucose. The large dynamic range is typical for GOX immobilized to SAMs on metal substrates [32,33]. The GOX monolayer and the GOX crosslinked (10 mg/mL) surfaces showed a similar current density response to the changes in glucose concentrations, with a current density of 1.0 ± 0.2 μA/cm^2 for the monolayer and 1.1 ± 0.3 μA/cm^2 for the crosslinked layer, at a glucose concentration of 50 mM. Although higher enzyme amounts were attached during the crosslinking method it apparently did not lead to a higher signal. These observations suggested to us that the glutaraldehyde-mediated cross-coupling results in partial deactivation of the enzyme, which is a known feature to occur during glutaraldehyde-mediated crosslinking [34]. When therefore higher enzyme concentrations were used during the GOX crosslinking immobilization procedure, and correspondingly lower relative amounts of glutaraldehyde, both the enzyme layer thickness (Table S2) and measured current ranges increased (Fig. S8). Using

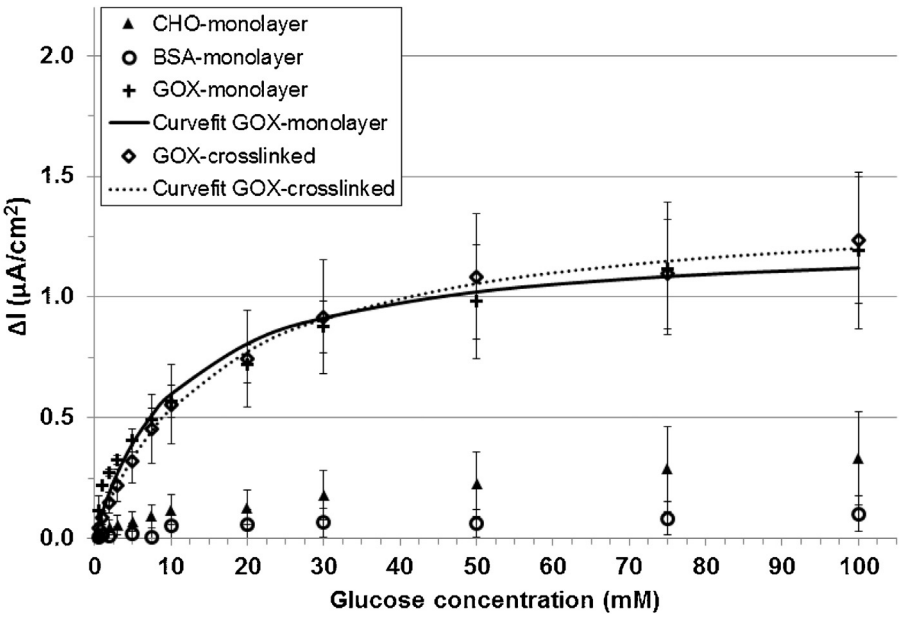

Fig. 6. Chronoamperometry results for the non-catalytic CHO-terminated monolayer, BSA-monolayer surfaces and the GOX coupled surfaces (GOX monolayer and GOX crosslinked). Data for surface-bound GOX were fitted to the Michaelis-Menten equation (Table 1).

Table 1
Kinetic constants derived by fitting the acquired chronoamperometric data to the Michaelis–Menten kinetic model of enzymatic reactions.

Source data	R^2	K_M (mM)	V_{max} ($\mu A\,cm^{-2}$)
GOX-monolayer	0.976	10.7	1.2
GOX-crosslinked	0.979	16.1	1.4
Soluble GOX [36]		25.7	
LOX-monolayer	0.999	0.37	1.02
Soluble LOX [37]		1.3	
Diluted layers LOX-monolayer	0.979	0.15	0.74
HAOX-layer by layer	0.987	1.85	0.73
Soluble HAOX [38]		16.5	

20 mg/mL GOX during cross-coupling resulted in an estimated enzyme layer thickness of 4.2 ± 1.2 nm and a detected current density of 2.1 ± 0.7 $\mu A/cm^2$ at a glucose concentration of 50 mM, while 50 mg/mL GOX resulted in a layer thickness of 4.7 ± 2.7 nm and 6.3 ± 4.0 $\mu A/cm^2$. The observed large variations in the detected current density and in the amount of immobilized enzyme for the surfaces prepared with 20 and 50 mg/mL GOX signify the low reproducibility of the glutaraldehyde crosslinking method. These current densities are about 2–3 times lower than those reported in the literature, but a straightforward explanation thereof is difficult, given both differences in substrate (thiols-on-Pt) [32] or thiols-on platinized gold [33] and the lack of e.g. enzyme layer thicknesses on both these papers. Still, our system shows more than acceptable current densities. For comparison, when 375 pmol of GOX was added to a solution of 100 mM glucose in buffer, a current density of 50.4 $\mu A/cm^2$ was measured using an unmodified PtOx electrode. The estimated amount of enzyme immobilized on the electrode is 2 pmol which produces a ΔI of 1 $\mu A/cm^2$ at a glucose concentration of 100 mM. So in our enzyme electrode system there is around 200 times less enzyme on the surface than in the solution experiment, but the current density is just 50 times smaller.

The GOX biosensor response currents were fitted using Michaelis-Menten kinetics (Fig. 6, Table 1). The calculated K_M values are in the same order of magnitude as the published values for soluble enzyme. The calculated K_M for the GOX monolayer is lower than for crosslinked GOX which indicates that GOX immobilized through the monolayer approach shows higher affinity for glucose than the crosslinked GOX. This is likely caused by a matrix effect, i.e. the partitioning of substrate into the immobilized enzyme layer is different for the two surfaces (the measured K_M is in fact an apparent K_M) [35].

The enzymatic films are stable towards H_2O_2, which was proven as follows. The enzyme-modified surface was divided in two parts: one was brought into contact with a buffered glucose solution while the other part was covered with buffer only. Subsequently, the chemical composition of both surfaces was analyzed by XPS and both analyses afforded the same results with a variation of ~1% in their chemical composition as determined by XPS.

3.3. *Covalent attachment of LOX and HAOX. Chronoamperometric evaluation of the activity of immobilized enzymes*

Next, the above developed methodology was applied to the covalent immobilization of LOX and HAOX onto functionalized Pt surfaces.

3.3.1. *Immobilization of LOX and electrochemical analysis of the attached enzymes*

The LOX monolayer attachment protocol onto CHO-functionalized Pt surfaces (Section 2.3.7, method A, Fig. 7A) afforded a thickness of immobilized enzyme of ~2.9 nm (Table S2) which corresponds to a surface enzyme loading $\Gamma \sim 4.9$ pmol.cm^{-2} (Eq. (5), molar mass of LOX 80×10^3 g mol^{-1}). The response of attached LOX was evaluated by chronoamperometry for lactate concentrations up to 20 mM. Immobilized LOX catalyzes the O_2 mediated conversion of lactate to pyruvate. In this process the O_2 is reduced to H_2O_2 which, upon application of 0.5 V, is oxidized on the PtOx surface generating a quantifiable electronic signal (current). Chronoamperometry measurements showed a reproducible relation between the observed current and the lactate concentration (0.05–20 mM, Fig. 7 and Fig. S10), with a current density of ~0.79 $\mu A/cm^2$ observed at 1.0 mM. Parra et al. [39] describe a similar dynamic range on lactate concentrations with current densities of the same order of magnitude for LOX covalently attached to 3,3-dithiodipropionic acid di(*N*-succinimidyl ester)-modified Au using hydroxymethylferrocene as an electron mediator. The response for the immobilized LOX-monolayer

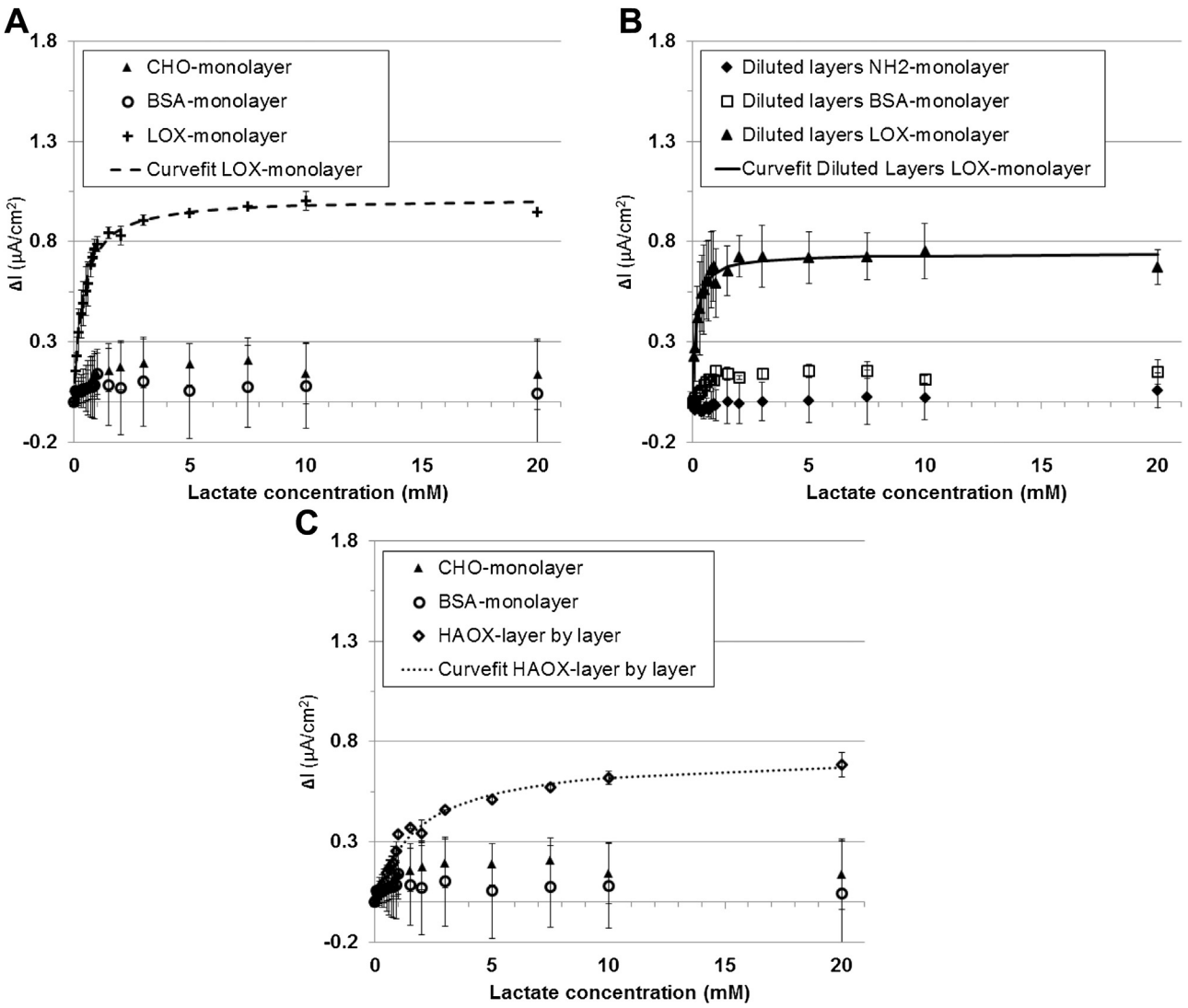

Fig. 7. Chronoamperometry results for (A) the LOX-terminated monolayer surface, (B) the diluted layer LOX-monolayer surface and (C) the HAOX layer-by-layer surface on lactate. Results of the associated control surfaces are given. All data were obtained from duplicate experiments. Data for surface-bound LOX and HAOX were fitted to the Michaelis-Menten equation (Table 1).

surface was significantly higher compared to the non-catalytic controls, indicating the successful immobilization of active LOX. In this regard the non-catalytic CHO-terminated and BSA-monolayer controls showed a similar response (Fig. 7). A maximal current density of ~0.21 μA/cm^2 was observed for the CHO-terminated surface and ~0.14 μA/cm^2 for the BSA-monolayer surfaces. These results reveal that LOX covalently attached to SAMs grafted on PtOx performs as a biosensor for lactate.

Crosslinking of LOX in the presence of glutaraldehyde (Section 2.3.7, method B) resulted in inactivation of the enzyme (Fig. S11). The crosslinking process can, as a result of multipoint attachment, lead to obstruction/deformation of the catalytic site or irreversible structural changes of the enzyme [35]. Therefore, and in order to further improve the activity of covalently attached LOX, we investigated the immobilization of LOX onto a surface containing a smaller number of anchoring points (Section 2.3.7, method C). This platform was produced by grafting PtOx surfaces with a mixture of 5-hexen-1-ol and, trifluoroacetamide-protected 10-amino-1-decene TFAAD in 10:1 ratio (thickness 0.90 nm, CA = 65 ± 3°, Scheme S1). 5-Hexene-1-ol was selected because it provided a thin monolayer that does not hamper the diffusion of H_2O_2 to the Pt surface. Moreover, the OH- groups of the organic monolayer possess a very low nucleophilic character, and are not expected to react with NHS-derived coupling agents in aqueous solutions. Trifluoroacetyl amide (TFAA) groups were hydrolyzed in basic media to thus produce OH-/NH_2- mixed monolayers (thickness 0.75 nm, CA = 63 ± 5°). Functionalization of the surface with sulfo-NHS moieties proceeded by reaction of the NH_2 groups with bis(sulfosuccinimidyl) suberate sodium salt (BS3) at room temperature in buffered solution. Finally, immobilization of LOX was accomplished by incubation of the activated surface with enzyme solution (3 mg/mL) for 45 min. The activity of attached enzyme was assessed as described previously. A maximal current density of ~0.07 μA/cm^2 was observed for the OH-/NH_2-terminated surface and ~0.15 μA/cm^2 for the BSA-monolayer surfaces. Current densities for the immobilized LOX-monolayer surface were higher compared to the non-catalytic controls, proving that the immobilized LOX remains active (Fig. 7B). The LOX-monolayer biosensor showed a stable relation between the observed current and lactate concentration (0.05–20 mM, Fig. 7 and Fig. S10), with a current density of ~0.59 μA/cm^2 observed at 1.0 mM. Surface enzyme loading and current densities on this platform are comparable to those obtained for LOX covalently attached to CHO surfaces. LOX biosensor response currents were fitted using

Michaelis-Menten kinetics (Fig. 7, Table 1). The K_M value for LOX on diluted monolayer is lower than for LOX attached to CHO surfaces.

3.3.2. Covalent attachment of HAOX. Chronoamperometric performance of immobilized enzymes

For biosensing applications in which there is direct contact between the sensor and body fluids, human enzymes are preferred over the bacterial ones such as GOX and LOX. The human enzyme that is most known for lactate oxidation is lactate dehydrogenase (EC 1.1.1.27), but this enzyme uses NADH as a substrate and therefore does not produce hydrogen peroxide. The human 2-hydroxyacid oxidase (HAOX EC 1.1.3.15) produces H_2O_2 and is also active on lactate, albeit with a low apparent k_{cat} (0.46 s^{-1}) and high K_m (16.6 mM) for this substrate [38]. We also explored the immobilization of this enzyme on Pt chips and we observed that, due to the low activity on lactate, large amounts of enzyme had to be immobilized in order to get measurable activity. Only a layer-by-layer approach (Section 2.3.7, method D) gave successful results (Fig. 7C, Table 1). In this protocol, after a first attachment of HAOX onto a CHO surface, two consecutive glutaraldehyde coupling and HAOX incubation steps were performed. This approach increased the amount of immobilized enzyme leading to a ~8.9 nm HAOX layer (Fig. S16), which yields a surface enzyme loading Γ of ~28 pmol cm^{-2} (using Eq. (5); molar mass of HAOX 43×10^3 g mol^{-1}). The resulting biosensor produced a current density of 0.68 μA/cm^2 at a lactate concentration of 20 mM. Remarkably, the (apparent) K_M value of the immobilized enzyme was ten times lower than the value for the soluble enzyme, showing a clear matrix effect, and thereby enabling the detection of lactate over a wide range of concentrations. To the best of our knowledge it is the first time that human HAOX is used for biosensing purposes and thus opens the possibility for in vivo sensing of lactate in humans which is fully compatible with the immune system.

4. Conclusions

Oxidase enzymes (LOX, GOX and human HAOX) were covalently attached onto alkene-based SAMs grafted on PtOx surfaces. SAMs were activated with aldehyde or NHS-ester groups to provide anchoring points for enzyme immobilization. Thus the PtOx surface served both as substrate for the SAM formation and enzyme immobilization, and as an electrochemical oxidation site of the catalytically produced H_2O_2 during the chronoamperometric analysis. Chronoamperometric measurements of SAMs on PtOx functionalized with enzymes demonstrate that covalently attached enzymes remain active. Covalent immobilization of GOX afforded glucose biosensors with a large dynamic range (0–50 mM glucose) that supported glucose concentration depended increase in current density. Lactate biosensors based on the attachment of LOX and HAOX showed a dynamic range with lactate concentration up to 1.0 mM and 10 mM lactate, respectively. Especially the results obtained with human HAOX open the possibility for a continuous in vivo lactate monitoring system in humans. The (apparent) affinity of the immobilized enzymes for their substrate is unaltered or even higher than the soluble enzymes. Our results demonstrate that covalently functionalized PtOx surfaces provide a highly suitable platform for the assembly of oxidase enzyme-based biosensors.

Acknowledgements

We thank Dr. Stefanie Lange for providing TFAAD, Dr. Anke Trilling for support in the preparation of TFE monolayers and Lionix BV for the generous gift of Pt surfaces. This work was funded by the GO-EFRO project Biomarque.

Appendix A. Supplementary data

Supplementary data associated with this article can be found, in the online version, at http://dx.doi.org/10.1016/j.apsusc.2016.05.006.

References

[1] C.R. Lowe, Biosensors. Trends Biotech. 2 (1984) 59–65.
[2] D. Grieshaber, R. MacKenzie, J. Voros, E. Reimhult, Electrochemical biosensors—sensor principles and architectures, Sensors 8 (2008) 1400–1458.
[3] D. Samanta, A. Sarkar, Immobilization of bio-macromolecules on self-assembled monolayers: methods and sensor applications, Chem. Soc. Rev. 40 (2011) 2567–2592.
[4] J.J. Gooding, S. Ciampi, The molecular level modification of surfaces: from self-assembled monolayers to complex molecular assemblies, Chem. Soc. Rev. 40 (2011) 2704–2718.
[5] N.K. Chaki, K. Vijayamohanan, Self-assembled monolayers as a tunable platform for biosensor applications, Biosens. Bioelectron. 17 (2002) 1–12.
[6] C. Vericat, M.E. Vela, G. Corthey, E. Pensa, E. Cortes, M.H. Fonticelli, F. Ibañez, G.E. Benitez, P. Carro, R.C. Salvarezza, Self-assembled monolayers of thiolates on metals: a review article on sulfur-metal chemistry and surface structures, RSC Adv. 4 (2014) 27730–27754.
[7] J.M. Alonso, B. Fabre, A.K. Trilling, L. Scheres, M.C.R. Franssen, H. Zuilhof, Covalent attachment of 1-alkenes to oxidized platinum surfaces, Langmuir 31 (2015) 2714–2721.
[8] J.P. Metters, F. Tan, R.O. Kadara, C.E. Banks, Platinum screen printed electrodes for the electroanalytical sensing of hydrazine and hydrogen peroxide, Anal. Methods 4 (2012) 1272–1277.
[9] Y. Xia, G.M. Whitesides, Soft lithography, Annu. Rev. Mater. Sci. 28 (1998) 153–184.
[10] A. Heller, B. Feldman, Electrochemical glucose sensors and their applications in diabetes management, Chem. Rev. 108 (2008) 2482–2505.
[11] S.P. Nichols, A. Koh, W.L. Storm, J.H. Shin, M.H. Schoenfisch, Biocompatible materials for continuous glucose monitoring devices, Chem. Rev. 113 (2013) 2528–2549.
[12] L. Rassaei, W. Olthuis, S. Tsujimura, E.J.R. Sudhölter, A. van den Berg, Lactate biosensors: current status and outlook, Anal. Bioanal. Chem. 406 (2014) 123–137.
[13] WHO, Global Status Report on Noncommunicable Diseases 2014, World Health Organization, Geneva, Switzerland, 2015.
[14] G.E. Fryxell, P.C. Rieke, L.L. Wood, M.H. Engelhard, R.E. Williford, G.L. Graff, A.A. Campbell, R.J. Wiacek, L. Lee, A. Halverson, Nucleophilic displacements in mixed self-assembled monolayers, Langmuir 12 (1996) 5064–5075.
[15] J. Veliscek-Carolan, K.A. Jolliffe, T.L. Hanley, Selective sorption of actinides by titania nanoparticles covalently functionalized with simple organic ligands, ACS Appl. Mater. Interfaces 5 (2013) 11984–11994.
[16] P.E. Laibinis, C.D. Bain, G.M. Whitesides, Attenuation of photoelectrons in monolayers of n-alkanethiols adsorbed on copper silver, and gold, J. Phys. Chem. 95 (1991) 7017–7021.
[17] M. Geissler, J. Chen, Y. Xia, Comparative study of monolayers self-assembled from alkylisocyanides and alkanethiols on polycrystalline Pt substrates, Langmuir 20 (2004) 6993–6997.
[18] M. Rosso, M. Giesbers, A. Arafat, K. Schroën, H. Zuilhof, Covalently attached organic monolayers on SiC and Si_xN_4 surfaces: formation using UV light at room temperature, Langmuir 25 (2009) 2172–2180.
[19] R. Arnold, W. Azzam, A. Terfort, C. Wöll, Preparation, modification, and crystallinity of aliphatic and aromatic carboxylic acid terminated self-assembled monolayers, Langmuir 18 (2002) 3980–3992.
[20] S. Margel, A. Rembaum, Synthesis and characterization of poly(glutaraldehyde). A potential reagent for protein immobilization and cell separation, Macromolecules 13 (1980) 19–24.
[21] Z. Li, P. Beck, D.A.A. Ohlberg, D.R. Stewart, R.S. Williams, Surface properties of platinum thin films as a function of plasma treatment conditions, Surf. Sci. 529 (2003) 410–418.
[22] M. Yang, R.L.M. Teeuwen, M. Giesbers, J. Baggerman, A. Arafat, F.A. de Wolf, J.C.M. van Hest, H. Zuilhof, One-step photochemical attachment of NHS-terminated monolayers onto silicon surfaces and subsequent functionalization, Langmuir 24 (2008) 7931–7938.
[23] J.T.C. Wojtyk, K.A. Morin, R. Boukherroub, D.D.M. Wayner, Modification of porous silicon surfaces with activated ester monolayers, Langmuir 18 (2002) 6081–6087.
[24] J. Piehler, A. Brecht, K. Hehl, G. Gauglitz, Protein interactions in covalently attached dextran layers, Colloids Surf. B 13 (1999) 325–336.
[25] H. Fischer, I. Polikarpov, A.F. Craievich, Average protein density is a molecular-weight-dependent function, Prot. Sci. 13 (2004) 2825–2828.
[26] P. Scodeller, F.J. Williams, E.J. Calvo, XPS analysis of enzyme and mediator at the surface of a layer-by-layer self-assembled wired enzyme electrode, Anal. Chem. 86 (2014) 12180–12184.
[27] D. Losic, J.G. Shapter, J.J. Gooding, Scanning tunneling microscopy studies of glucose oxidase on gold surfaces, Langmuir 18 (2002) 5422–5428.

[28] G.O. de Benedetto, C. Malitesta, C.G. Zambonin, Electroanalytical/X-ray photoelectron spectroscopy investigation on glucose oxidase adsorbed on platinum, J. Chem. Soc. Faraday Trans. 90 (1994) 1495–1499.
[29] A.J. Guiomar, J.T. Guthrie, S.D. Evans, Use of mixed self-assembled monolayers in a study of the effect of the microenvironment on immobilized glucose oxidase, Langmuir 15 (1999) 1198–1207.
[30] A. Barth, C. Zscherp, What vibrations tell about proteins, Q. Rev. Biophys. 35 (2002) 369–430.
[31] S. Park, H. Boo, T.D. Chung, Electrochemical non-enzymatic glucose sensors, Anal. Chim. Acta 556 (2002) 46–57.
[32] X.D. Dong, J.T. Lu, C.S. Cha, Study of glucose-oxidase on Pt electrode modified by alkane thiol, Bioelectrochem. Bioenerg. 36 (1995) 73–76.
[33] J.J. Gooding, V.G. Praig, E.A.H. Hall, Platinum-catalyzed enzyme electrodes immobilized on gold using self-assembled layers, Anal. Chem. 70 (1998) 2396–2402.
[34] I. Migneault, C. Dartiguenave, M.J. Bertrand, K.C. Waldron, Glutaraldehyde: behavior in aqueous solution, reaction with proteins, and application to enzyme crosslinking, BioTechniques 37 (2004) 790–802.
[35] A. Liese, L. Hilterhaus, Evaluation of immobilized enzymes for industrial applications, Chem. Soc. Rev. 42 (2013) 6236–6249.
[36] F. Gao, O. Courjean, N. Mano, An improved glucose/O_2 membrane-less biofuel cell through glucose oxidase purification, Biosens. Bioelectron. 25 (2009) 356–361.
[37] R. Kataky, R.M. Zawawi, Modification of the chiral selectivity of D-glucose oxidase and L-lactate oxidase in a collagen matrix, Phys. Chem. Chem. Phys. 12 (2010) 9183–9187.
[38] C. Vignaud, N. Pietrancosta, E.L. Williams, G. Rumsby, F. Lederer, Purification and characterization of recombinant human liver glycolate oxidase, Arch. Biochem. Biophys. 465 (2007) 410–416.
[39] A. Parra, E. Casero, L. Vazquez, F. Pariente, E. Lorenzo, Design and characterization of a lactate biosensor based on immobilized lactate oxidase onto gold surfaces, Anal. Chim. Acta 555 (2006) 308–315.